PCCP

PAPER

A comparative analysis of the UV/Vis absorption spectra of nitrobenzaldehydes†

Verónica Leyva,[a] **Inés Corral,**[*b] **Thomas Schmierer,**[cd] **Peter Gilch**[cd] **and Leticia González***[a]

In a joint experimental and theoretical study, the UV/Vis absorption spectra of the three isomers (*ortho*, *meta*, *para*) of nitrobenzaldehyde (NBA) were analyzed. Absorption spectra are reported for NBA vapors, cyclohexane and acetonitrile solutions. All spectra are poor in vibronic structure and hardly affected in shape by the surroundings (vapor or solution). Moderate solvatochromic shifts of ~ -0.2 eV are measured. For all isomers vertical transition energies, oscillator strengths, and excited state dipole moments were computed using the MS-CASPT2/CASSCF and CC2 methods. Based on these calculations the experimental transitions were assigned. The spectra of all isomers are characterized by weak ($\varepsilon_{max} \approx 100$ M^{-1} cm^{-1}) transitions around 350 nm (3.6 eV), arising from nπ* absorptions starting from the lone pairs of the nitro and aldehyde moieties. The next band of intermediate intensity peaking around 300 nm (4.2 eV, $\varepsilon_{max} \approx 1000$ M^{-1} cm^{-1}) is dominated by $\pi\pi$* excitations within the arene function. Finally, strong absorptions ($\varepsilon_{max} \approx 10\,000$ M^{-1} cm^{-1}) were observed around 250 nm (5.0 eV) which we ascribe to $\pi\pi$* excitations involving the nitro and benzene groups.

1. Introduction

The substitution pattern of nitrobenzenes strongly affects their photoreactivity. While *meta*(*m*)- and *para*(*p*)-substituted nitrobenzenes are usually photochemically inert, the *ortho*(*o*)-derivatives commonly photoreact with high quantum yields provided that the substituent contains hydrogen atom(s).[1] The obvious rationale for this observation is that photoexcitation triggers a transfer of a hydrogen atom from the *ortho*-substituent to the nitro group. The transfer is ensued by further reactions which eventually result in the formation of the photoproduct. For *o*-nitrobenzaldehyde (*o*-NBA) femto-second spectroscopy showed that this transfer involves excited singlet and triplet states.[2–5] The transfer *via* the singlet channel is dominant and occurs on the time scale of some 100 fs.[4] In a comparative study[3] on all three isomers of nitrobenzaldehyde it has been shown that the reactive isomer (*o*-NBA) does not differ substantially from the non-reactive isomers in terms of

fluorescence decay patterns. For all isomers photoexcitation to an upper singlet state results in an ultrafast ($<$100 fs) decay of the fluorescence emission. A slower component ($\sim$0.5–1 ps) of the decay carries only a very small amplitude (0.01 of the initial signal). The tentative interpretation of this observation has been that an initially excited (bright) $\pi\pi$* state decays *via* internal conversion and populates a "darker" nπ* state.[3] Hydrogen transfer (*o*-NBA) and/or intersystem crossing (*o,m,p*-NBA) in turn depopulate this state.

We are presently working on a firmer interpretation based on high-level quantum chemistry and quantum dynamics. As a part of this effort, we here present a joint experimental and theoretical study on the vertical excitation energies and oscillator strengths of nitrobenzaldehydes. This work is an extension of an earlier investigation[6] focusing on *o*-NBA only. For the sake of completeness these results will be briefly reviewed below. The paper is organized as follows. Absorption spectra of the three isomers as vapors and in cyclohexane and acetonitrile solutions will be presented. These environments were chosen for two reasons. Vapor spectra were recorded to facilitate the comparison with the quantum chemical computations which were conducted for vacuum conditions. Further measured solvatochromic shifts should show trends on the changes of dipole moments upon excitation. Then the electronic ground state of the three isomers will be characterized in terms of equilibrium geometries by means of quantum chemical computations. Thereby, also the issue of conformational variety and aromaticity will be addressed. Based on the computed

[a] *Institut für Physikalische Chemie, Friedrich-Schiller-Universität Jena, Helmholtzweg 4, 07743 Jena, Germany*
[b] *Departamento de Química C-9, Universidad Autónoma de Madrid, Cantoblanco, 28049 Madrid, Spain*
[c] *Fakultät für Physik, Ludwig-Maximilians-Universität München, Oettingenstr. 67, 80538 München, Germany*
[d] *Institut für Physikalische Chemie, Heinrich-Heine-Universität Düsseldorf, Universitätsstr. 1, 40225 Düsseldorf, Germany*
† Electronic supplementary information (ESI) available: Full assignment (including molecular orbitals) of the MS-CASPT2/CASSCF and CC2 vertical spectra. See DOI: 10.1039/c0cp01372b

This journal is © the Owner Societies 2011

Phys. Chem. Chem. Phys., 2011, **13**, 4269–4278 | 4269

geometries, vertical excitation energies, oscillator strengths, and permanent dipole moments in the excited state will be evaluated. These computational results will then be compared with the experimental spectra to arrive at a consistent assignment of the transitions responsible for the UV/Vis spectra.

2. Experimental methods

All experimental spectra presented were measured with a commercial dual beam spectrograph (Perkin Elmer, Lambda 19). Cyclohexane (Merck, Uvasol) and acetonitrile (Sigma Aldrich, spectrophotometric grade, ≥ 99.5 %) were used as solvents. *o*-Nitrobenzaldehyde was purchased from Merck, *m*- and *p*-NBA from Sigma-Aldrich. All of them were used as received. For the solution spectra the samples were held in 1 mm fused silica cells. Typical concentrations were in the range of 0.3–1 mM. To obtain gas phase spectra a heatable home-built cell was used. This cell was of cylindrical shape and featured a path length of 10.4 cm. Front and back of the cylinder consisted of a double layer of optical windows (fused silica) with a spacing of ∼1 mm in between. The cylindrical body of the cell was encircled by a brazen pipe. Water with a temperature of 90 °C was flown through the pipe to heat up the nitrobenzaldehyde sample and generate a vapor pressure sufficient to obtain spectra. The hot water also flowed through the spacing of the front and back windows. Thereby crystallization of the sample on the windows was prevented. Typical optical densities at absorption maxima were of the order of 0.1–0.5.

3. Computational details

Ground state structures for the isomers were optimized before computing the UV spectra. The optimization in the electronic ground state relied on density functional calculations using the B3LYP functional and the 6-311G(d,p) basis set. This level of theory demonstrated for *o*-NBA[6] a good agreement with the available X-ray geometry.[7] The B3LYP approach includes Becke's three parameter hybrid exchange potential[8] and the Lee–Yang–Parr correlation functional.[9] The optimizations were performed with GAUSSIAN-03 suite programs.[10]

An energy decomposition analysis (EDA) has been performed to estimate the effect of the substituents on the aromaticity of the system in the ground state. A detailed description of this method can be found *e.g.* in ref. 11–14. EDA can provide useful information on the π conjugation and the nature of the bonds[15] or even explain the way the position of the substituents can influence a reaction site through resonance and field/inductive effects.[16] EDA calculations have been performed at the BP86/ TZ2P level of theory[17–19] and the ADF code[12,20,21] fragmenting the system into three parts: the benzene ring, the aldehyde and the nitro group.
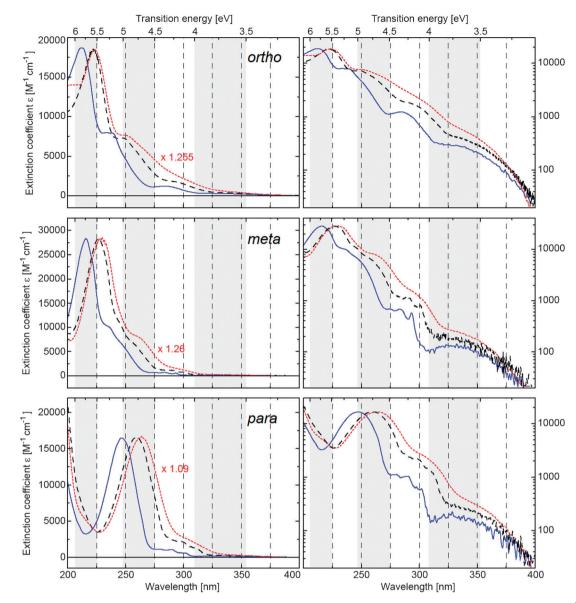
The vertical UV absorption spectra have been calculated on the optimized geometries by means of the second order coupled cluster (CC2) method[22] and the multi-state second order perturbation theory[23] on complete active space self consistent field wave functions[24] (MS-CASPT2/CASSCF). MS-CASPT2/CASSCF prescription has been shown to be one of the most accurate ones to calculate excitation energies,

with errors ranging from 0.1 to 0.3 eV.[25] Errors in the calculation of the oscillator strengths are much more difficult to quantify. Guided by the results obtained in our earlier study on *o*-NBA[6] the CAS reference wave functions have been built with two different active spaces, namely 16 electrons in 12 orbitals (16,12) and 12 electrons in 11 orbitals (12,11). The (16,12) active space aims to describe the nπ* transitions starting from the lone pairs of the nitro and aldehyde groups. Therefore, it includes three lone pairs, two from the nitro group and one from the aldehyde group, and additionally two pairs of π_{CC}/π^*_{CC} orbitals from the benzene ring, one pair of π_{CO}/π^*_{CO} from the aldehyde group, one pair of π_{NO2}/π^*_{NO2}, and a non-bonding π orbital P_{NO2} from the nitro group (see Fig. S1 and S2, ESI†). Since it is not possible to include the whole π system and the lone pairs in the same active space, we designed the smaller (12,11) active space to account for the high energy ππ* transitions at the expense of excluding the lone pairs. Specifically, this active space includes three π_{CC}/π^*_{CC} pairs from the aromatic moiety, one pair of π_{CO}/π_{CO}^* from the aldehyde group, the pair of π_{NO2}/π^*_{NO2}, and the non-bonding π orbital P_{NO2} from the nitro group. The calculations for the *p*- and *m*-NBA isomers are done within C_s symmetry, while the earlier calculation for *o*-NBA was performed without symmetry.[6] Accordingly, the (16,12) active space calculations were performed as one root for the ground state of A′ symmetry and as state-average (SA) over three roots for the electronic excited states of A″ symmetry (nπ* excitations). The (12,11) calculations were done with state averaging over 4 roots of A′ symmetry, which includes the ground state and three ππ* excited states. The weight is the same for all the states considered.

The dynamical correlation has been introduced by means of the second order perturbation theory on the SA-CASSCF wave functions. To remedy the appearance of intruder states, the level-shift technique[26] with a parameter of 0.3 a.u. has been used. Oscillator strengths have been obtained with the RAS state interaction method (RASSI)[27] using MS-CASPT2 energies and perturbation modified CAS (PM-CAS) transition dipole moments. The large atomic natural orbital basis set ANO-L,[28] contracted as C,O,N[4s3p2d]/H[3s2p], has been employed in all the multiconfigurational calculations. MS-CASPT2/CASSCF and CC2 vertical excited spectra have been computed using MOLCAS 6.0 software[29] and the Turbomole package,[30] respectively.

4. Experimental results

The spectra of the three isomers exhibit many commonalities so their properties will be described jointly; differences among them are mentioned on the way. The nitrobenzaldehydes start absorbing at wavelengths smaller than 400 nm (3.1 eV), see Fig. 1. In the spectral range of 200–400 nm (6.20–3.10 eV) four bands are directly discernible (by the band shape analysis described below more bands will be resolved). Their peak extinction increases with decreasing wavelength. The bands of lowest transition energy are centered at ∼350 nm (3.6 eV). Their extinction coefficients at the peak are of the order of 100 M^{-1} cm^{-1}. These lowest energy bands do not exhibit any vibronic structure. The bands second lowest in energy peak

Fig. 1 UV/Vis absorption spectra of the three isomers of nitrobenzaldehyde in different surroundings. The extinction coefficients in M^{-1} cm^{-1} are plotted *versus* a linear wavelength axis (lower *x*-axis). An energy scale is given by the upper *x*-axis. In the spectra on the left the extinction axis is linear, on the right it is logarithmic to highlight weaker transition. For the sake of comparison all spectra were normalized to the peak value of NBA dissolved in cyclohexane (black dashed line). The necessary scaling factor for NBA in acetonitrile (red dotted line) is given in the graph. For the NBA vapour (blue solid line) the scaling factor in terms of extinction coefficient could not be evaluated.

around 300 nm (4.2 eV) and exhibit extinction coefficients of around 1000 M^{-1} cm^{-1}. For the *meta*- and *para*-isomers a vibronic progression is observed in non-polar surroundings. Around 250 nm (5.0 eV) bands with extinction coefficients of $\sim 10\,000$ M^{-1} cm^{-1} are located. These bands lack a vibronic structure. The bands highest in energy in the spectral range covered are centered at ~ 225 nm (5.6 eV)—except for the *para*-isomer, for which it is located at wavelengths smaller than 200 nm (6.2 eV). The extinction coefficients exceed 10 000 M^{-1} cm^{-1} and the bands are structureless. Gas phase and solution spectra are very similar in shape. The same observation has been made for nitrobenzene[31] and *o*-ethylnitrobenzene.[6] This suggests that intramolecular mechanisms mostly hold responsible for broad spectral features. With increasing

polarity (gas phase, cyclohexane, and acetonitrile) all bands move to longer wavelengths, *i.e.* the bands exhibit positive solvatochromism.

For a more quantitative assessment of band positions, solvent shifts, and oscillator strengths, the experimental spectra were subjected to a fitting procedure using a sum of Gaussians as trial functions (for the justification of this approach see ref. 6). It has to be stressed that a Gaussian is only an approximation for the true vibronic envelope of an electronic transition. It may well be that more than one Gaussian is required for the description of the envelope or that two transitions are described by one Gaussian. Thus, the statement "one Gaussian stands for one transition" must not be made. Fitting of the spectra required 7–8 Gaussians. In our
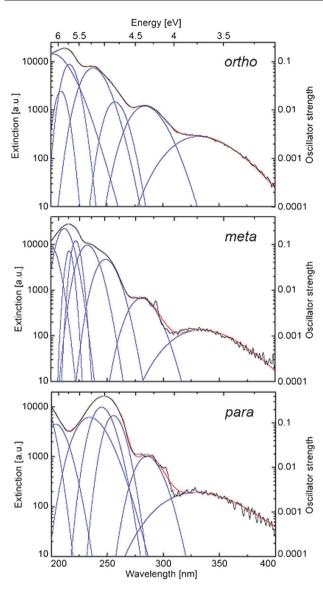
Fig. 2 Gaussian decomposition of the UV/Vis absorption spectra (black lines) of the three NBA isomers as vapours. The extinction coefficients were obtained by scaling the measured absorption spectra so that the highest vapour extinction equals the highest value in cyclohexane solution (*cf.* Fig. 1). The Gaussian components are represented by blue lines, their sum by the red lines. Note that the *y*-axis is logarithmic.

previous analysis[6] on *o*-NBA in solution (acetonitrile) 6 Gaussians sufficed to describe the spectrum. For the present vapor spectrum, which exhibits more structure, a better description is obtained using 7 Gaussians. The quality of the fits for vapor data can be assessed from Fig. 2 and the numerical results for all environments are compiled in Table 1. The oscillator strength f_i for each Gaussian is based on the following equation:[32]

$$f_i = 4.32 \times 10^{-9} \int \varepsilon_i(\tilde{v}) d\tilde{v} \qquad (1)$$

Hereby, ε_i is the extinction coefficient of the Gaussian component measured in units $M^{-1}\,cm^{-1}$ as a function of the wavenumber $\tilde{v}$ in cm^{-1}. The values refer to one Gaussian, *i.e.* not necessarily to one electronic transition. Since for the NBA vapors concentrations were not determined, extinction coefficients and thereby oscillator strengths f_i could not be calculated. The oscillator strengths f_i given in Table 1 were determined for cyclohexane solutions.

For all three isomers one determines Gaussians centered around 3.8 eV (vapour value) featuring oscillator strengths of ∼0.01. A second Gaussian with a comparable strength is located at 4.3 eV. The third Gaussian at ∼4.8 eV exceeds these strengths by roughly one order of magnitude. Whereas for the first three Gaussians all isomers resemble each other, stronger differences are observed for those located at higher energies. The fourth Gaussians of *o*-NBA and *m*-NBA are centered on 5.3 eV, the *o*-NBA Gaussian being by a factor of three higher in oscillator strength. For *p*-NBA the fourth Gaussian is lower in energy (5.06 eV) and carries substantial oscillator strength. Differences are more pronounced for the fifth Gaussian being located at 5.73 eV (f_5 = 0.098, *o*-NBA), 5.59 eV (0.009, *m*-NBA), and 5.29 eV (0.100, *p*-NBA). The sixth Gaussian represents a rather strong transition ($f \approx 0.15$) and peaks around ∼5.9 eV. Values for the seventh Gaussian are subject to a substantial error for *o*-NBA and *p*-NBA since their maxima are located outside the spectral range covered. For *m*-NBA a Gaussian with a larger oscillator strength of 0.420 peaks at 5.86 eV.

The positions of all Gaussians experience solvatochromic shifts. Except for the first Gaussians and the Gaussians at the high energy edge of the spectrum the following trend is observed. Going from gas phase to cyclohexane solution causes a peak shift of ∼−0.2 eV (*i.e.* to lower energies). Going to the more polar solvent, acetonitrile, induces an additional

Table 1 Compilation of the results from the Gaussian decomposition of the spectra of the three isomers depicted in Fig. 1. The centres of the Gaussians are given in eV. The respective oscillator strengths for the NBA isomers dissolved in cyclohexane were computed using eqn (1)

	ortho				meta				para			
No.	Vapour (eV)	Cyclohexane (eV)	Oscillator strength	Acetonitrile (eV)	Vapour (eV)	Cyclohexane (eV)	Oscillator strength	Acetonitrile (eV)	Vapour (eV)	Cyclohexane (eV)	Oscillator strength	Acetonitrile (eV)
1	3.73	3.74	0.011	3.61	3.72	3.88	0.008	3.67	3.76	3.63	0.006	3.61
2	4.37	4.21	0.022	4.21	4.42	4.27	0.011	4.26	4.34	4.17	0.028	4.11
3	4.82	4.76	0.083	4.70	4.99	4.86	0.110	4.68	4.85	4.61	0.090	4.55
4	5.22	5.03	0.047	4.96	5.34	5.06	0.016	5.06	5.06	4.84	0.190	4.79
5	5.73	5.48	0.098	5.48	5.59	5.31	0.009	5.28	5.29	5.14	0.100	5.05
6	5.93	5.65	0.170	5.66	5.74	5.42	0.230	5.42	6.08	5.84	0.110	6.03
7	6.14	6.28	—	6.09	5.86	5.61	0.420	5.74	6.48	6.40	—	6.31
8					6.21	6.91	—	6.32				

shift of −0.05 eV. The observation that a larger shift is caused for the change of gas phase to unpolar solvent as compared to the change of unpolar to polar solution is in line with predictions of a Lippert–Mataga treatment.[33] In principle such a treatment can afford dipole moments of excited states. Yet, to deduce dipole moments from the experimental data they need to be parallel for ground and excited states—otherwise the problem is under-determined. For none of the isomers symmetry fixes the direction of the dipole moment and therefore the moments of different states do not need to be parallel. Indeed, the quantum chemical calculations described below show that the directions of the dipole moments differ. A treatment based on *the assumption* that the dipole moments are parallel predicts dipole moments of the excited states which are by 2–3 D larger than that of the ground state.
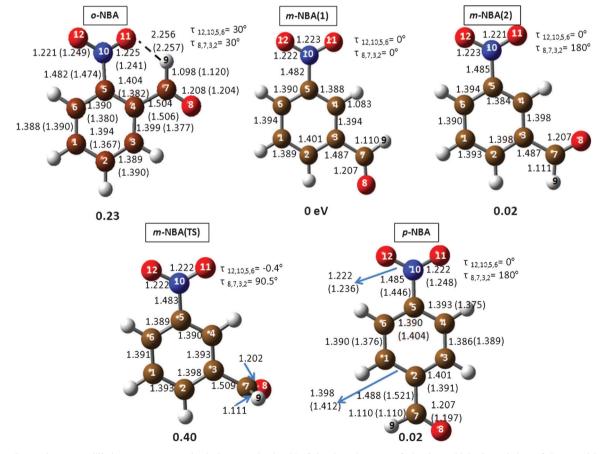
5. Computational results

5.1 Ground state equilibrium structures

Transition energies were computed on the ground state geometries obtained at the B3LYP/6-311G(d,p) level of theory. The optimized structures will be compared with diffraction data when available. X-ray structures have been reported for the *ortho*-[7] and *para*-[34] isomers. To our knowledge, there are no diffraction data on *m*-NBA. A detailed description of

the *o*-NBA structure can be found in ref. 6. Briefly, DFT calculations and diffraction data[7,35] agree that the hydrogen atom of the aldehyde substituent points to the nitro group (see Fig. 3). *o*-NBA adopts a non-planar structure. The angle which the nitro group and the benzene plane span amounts to 30° and the angle between the aldehyde function and the ring equals 30°. This distortion is the result of a balance between minimizing the steric hindrance of the NO$_2$ and CHO groups while forming a hydrogen bond between both fragments. Note that although the existence of this hydrogen bond has been questioned in the literature,[35,36] a topographic analysis of the charge density in *o*-NBA reveals a clear interaction between the O atom of the nitro group and the aldehyde hydrogen in the gas phase structure.[37] Also as a consequence of these two effects, the C$_4$–C$_5$ bond distance in *o*-NBA stretches by almost 0.02 Å, as compared to the other isomers.

For the *meta*-isomer one expects two conformers which differ in the orientation of the aldehyde group. The two conformers, labelled *m*-NBA(1) and *m*-NBA(2), are interconnected through the rotation of the C$_3$–C$_7$ single bond, passing *via* a transition state, *m*-NBA(TS), at an intermediate angle. Both conformers are planar. In line with an earlier investigation[38] the two conformers are energetically almost degenerate (see Fig. 3), *m*-NBA(2) being just 0.02 eV less stable than *m*-NBA(1). Assuming a negligible difference in

Fig. 3 Ground state equilibrium geometry and relative energies in eV of the three isomers of nitrobenzaldehyde and that of the transition state connecting the two *meta*-conformers as obtained from B3LYP/6-311G(d,p) optimisations. Values in parentheses correspond to experimental values when available.[7,34] Bond distances are in angstroms and bond angles in degrees.

entropy this indicates that at room temperature both conformers co-exist. Consequently, both will contribute to the same extent to the UV absorption spectrum. The height of the energy barrier associated with the TS ($170i$ cm^{-1}) amounts to 0.40 eV with respect to the most stable conformer, m-NBA(1). The interconversion between the two conformers should thus be slow on spectroscopic time scales. The slightly higher stability of the m-NBA(1) isomer compared to m-NBA(2) could be explained in terms of the electrostatic interactions between the oxygen atoms of the NO$_2$ or carbonyl groups and their adjacent hydrogens. The m-NBA(1) and m-NBA(2) are structurally very similar. The out-of-plane distortion of the aldehyde fragment in the TS leads to a slightly stretched C$_3$–C$_7$ distance by 0.022 Å compared to the planar molecules.

As in the two $meta$-isomers, the nitro and aldehyde groups of the $para$-isomer are coplanar with the plane of the arene ring, in agreement with the X-ray structure.[34] The $para$-isomer lies at $ca.$ 0.02 eV above the most stable m-NBA(1) isomer. Its geometry is very similar to that of the m-NBA isomers. In comparison to the $ortho$-isomer, the most significant differences are found in the C–C bond that connects the aldehyde group with the arene ring. This bond is shorter in p- and m-NBA, and therefore stronger, due to the lack of the hydrogen bond present in o-NBA.[37]

Quite interesting is the comparison of the structure of the aldehyde group for all the isomers. While one would expect the $ortho$-isomer to have the largest C$_7$–H$_9$ distance, since it participates in the hydrogen bond with the NO$_2$ group, m-NBA(1), m-NBA(2) and p-NBA exhibit C–H bonds longer by 0.015 Å with respect to o-NBA. Once more, it is the balance between the strength of the intramolecular hydrogen bond and the steric constraints between the two substituents that conditions the geometry of the aldehyde group.

After discussing the relative energies and geometrical differences of the three isomers, it is useful to compare them in terms of aromaticity. Below we summarize the results of the EDA on the $ortho$-, $meta$-, and $para$-substituted NBA, see Table 2. The total interaction energy ΔE_{int} corresponds to the sum of the electrostatic, Pauli repulsion and orbital terms, ΔE_{elstat}, ΔE_{Pauli} and ΔE_{orb}. The ΔE_{orb} energy can be partitioned into the σ and π bonding contributions, ΔE_σ and ΔE_π. Since o-NBA is not planar, the partition of ΔE_{orb} into its

π- and σ-components was not possible for this isomer. From the examination of the obtained energies it appears that σ contributions are much larger than π, indicating that the σ-bonding is stronger than π-bonding in all isomers. Moreover, we observe that the ΔE_π energies for the $para$- and $meta$-isomers are very similar. Therefore, no significant differences due to conjugation effects are expected in the spectra of the three isomers ($vide$ $infra$).

5.2 Computed vertical transition energies and spectral assignment

In order to assign the experimental bands, gas phase vertical excitation energies with their corresponding oscillator strengths have been computed at the CC2 and MS-CASPT2 levels of theory. The results from the Gaussian decomposition of the experimental spectra for the three NBA isomers are compiled in Table 1. Tables 3, 4 and 5 collect the results obtained with CC2 and MS-CASPT2 theories. The involved orbitals of the $meta$- and $para$-isomers are shown in Fig. S1 and S2, ESI.†

For completeness, we briefly review here the absorption spectrum of o-NBA,[6] see Table 3. Although the values obtained with CC2 and MS-CASPT2 are not identical, general statements regarding the interpretation of the spectrum of the three isomers can be made. The lowest part of the spectrum is characterized by nπ* absorptions from the NO$_2$ and CHO groups, appearing at energies below $ca.$ 4.2 eV. (Energies referring to theoretical values are denoted as eV$_t$, experimental values eV$_e$.) In the following experimental values are vapour phase transition energies and oscillators strengths based on fitting the cyclohexane spectra ($cf.$ Table 1). Both types of computations assign the weak and broad low energy band to the S$_1$–S$_3$ transitions. The S$_4$ and S$_5$ are $\pi\pi$* excitations at the MS-CASPT2 level of theory, responsible for the band at 4.96 eV$_e$. CC2 intercalates one additional state, which allows to associate one-to-one the three experimental Gaussians at 4.37, 4.82 and 5.22 eV$_e$ with S$_4$, S$_5$ and S$_6$. The most intense band is centred at 5.93 eV$_e$ and it is characterized by an excitation within the NO$_2$ group and calculated at 5.55 eV$_t$ by MS-CASPT2 and at 6.20 eV$_t$ by CC2.

Similar to o-NBA, the lowest energy region of the spectra of m-NBA and p-NBA is composed of one weak band peaking in the experiment at 3.72 eV$_e$ and 3.76 eV$_e$ which we ascribe to nπ* transitions (see Tables 4 and 5). These bands are assigned to the S$_1$, S$_2$, and S$_3$ states of the two conformers, m-NBA(1) and m-NBA(2), as well as to the same states for p-NBA. In m- and p-NBA, our calculations, at both levels of theory, yield transitions of nπ* character whereby n orbitals, located at the nitro as well as the carbonyl function, are involved. The electron accepting π* orbitals are situated at the nitro and carbonyl functions as well as at the benzene ring ($cf.$ Tables S1 and S2 and Fig. S1 and S2 in the ESI†). Since vibronic couplings are not incorporated in the theoretical calculations, negligible oscillator strengths for the nπ* states of the planar $meta$- and $para$-isomers are obtained.

We assign the band at 4.42 eV$_e$ to the sum of the S$_4$ states of the two conformers of m-NBA, which are theoretically predicted to absorb around 4.30 eV$_t$ or 4.83 eV$_t$ at MS-CASPT2 and

Table 2 Energy decomposition analysis for o-, m- and p-NBA at the BP86/TZ2P//B3LYP/6-311G(d,p) level of theory. Energies are in eV

	o-NBA	m-NBA(1)	m-NBA(2)	p-NBA
ΔE_{Int}/eV	−6.77	−7.55	−7.50	−8.04
ΔE_{Pauli}/eV	31.30	32.18	31.99	34.31
$\Delta E_{elstat}{}^a$/eV	−13.63	−14.45	−14.38	−15.54
%	35.8	36.4	36.4	36.7
$\Delta E_{orb}{}^a$/eV	−24.43	−25.28	−25.12	−26.81
%	64.2	63.6	63.6	63.3
$\Delta E_\sigma{}^b$/eV	—	−23.75	−23.68	−25.31
%	—	93.9	94.0	94.4
$\Delta E_\pi{}^b$/eV	—	−1.53	−1.50	−1.50
%	—	6.1	6.0	5.6

^{a} The percentages give the contribution to the total attractive ΔE_{elstat} + ΔE_{orb}. ^{b} The percentages give the contribution to the orbital interactions ΔE_{orb}.

Table 3 MS-CASPT2/CASSCF and CC2 excitation energies ΔE (in eV and nm), oscillator strengths f, and results of the Gaussian decomposition of the experimental spectrum of o-NBA

o-NBA

MS-CASPT2/CASSCF			RI-CC2			Assignment	Experiment		
States	ΔE (eV, nm)	f	States	ΔE (eV, nm)	f		Gauss center (eV, nm)		f
S_1	3.33	372	0.00	S_1	3.62	343	0.012	n → π*	3.73	332	0.011
S_2	3.82	324	0.00	S_2	4.09	303	0.001	n → π*			
S_3	3.88	319	0.00	S_3	4.11	301	0.004	n → π*			
S_4	4.45	278	0.01	S_4	4.57	271	0.007	π → π*	4.37	284	0.022
—				S_5	4.95	250	0.015	n → π*	4.82	257	0.083
S_5	4.94	251	0.23	S_6	5.30	234	0.134	π → π*	5.22	238	0.047
—				S_7	5.82	213	0.087	π → π*	5.73	216	0.098
S_6	5.55	223	0.05	S_8	6.20	200	0.142	P_{NO2} → π*/π → π*	5.93	209	0.170
				S_9	6.21	200	0.204	P_{NO2} → π*/π → π*	6.14	202	—

MS-CASPT2/CASSCF States	ΔE (eV)	nm	f	RI-CC2 States	ΔE (eV)	nm	f	Assignment	Gauss center (eV)	nm	f
S_1	3.33	372	0.00	S_1	3.62	343	0.012	n → π*	3.73	332	0.011
S_2	3.82	324	0.00	S_2	4.09	303	0.001	n → π*			
S_3	3.88	319	0.00	S_3	4.11	301	0.004	n → π*			
S_4	4.45	278	0.01	S_4	4.57	271	0.007	π → π*	4.37	284	0.022
—				S_5	4.95	250	0.015	n → π*	4.82	257	0.083
S_5	4.94	251	0.23	S_6	5.30	234	0.134	π → π*	5.22	238	0.047
—				S_7	5.82	213	0.087	π → π*	5.73	216	0.098
S_6	5.55	223	0.05	S_8	6.20	200	0.142	P_{NO2} → π*/π → π*	5.93	209	0.170
				S_9	6.21	200	0.204	P_{NO2} → π*/π → π*	6.14	202	—

Table 4 MS-CASPT2/CASSCF and CC2 excitation energies ΔE (in eV and nm), oscillator strengths f, and results of the Gaussian decomposition of the experimental spectrum of m-NBA

m-NBA(1) MS-CASPT2/CASSCF States[a]	ΔE (eV, nm)	f	RI-CC2 States	ΔE (eV, nm)	f	Assignment	m-NBA(2) MS-CASPT2/CASSCF States[a]	ΔE (eV, nm)	f	RI-CC2 States	ΔE (eV, nm)	f	Assignment	m-NBA Experiment Gauss center (eV, nm)	f
S_1	3.63 341	0.000	S_1	3.92 316	0.000	n → π*	S_1	3.60 344	0.000	S_1	3.93 315	0.000	n → π*	3.72 334	0.008
S_2	3.74 331	0.000	S_2	4.00 310	0.000	n → π*	S_2	3.69 336	0.000	S_2	4.00 310	0.000	n → π*		
S_3	4.16 298	0.000	S_3	4.58 271	0.000	n → π*	S_3	4.13 300	0.000	S_3	4.57 271	0.000	n → π*		
S_4	4.29 289	0.002	S_4	4.83 257	0.010	π → π*	S_4	4.30 288	0.001	S_4	4.83 256	0.003	π → π*	4.42 281	0.011
—			S_5	5.58 222	0.000	n → π*	—			S_5	5.54 224	0.000	n → π*	4.99 249	0.110
S_5	5.02 247	0.159	S_6	5.63 220	0.106	π → π*	S_5	5.43 229	0.051	S_6	5.79 214	0.081	π → π*	5.34 232	0.016
—			S_7	6.12 203	0.436	π → π*	—			S_7	6.09 204	0.591	π → π*	5.59 222	0.009
—			S_8	6.33 196	0.000	n → π*	—			S_8	6.19 200	0.000	n → π*	5.74 216	0.230
S_6	5.74 216	0.031	S_9	6.35 195	0.285	P_{NO2} → π*/π → π*	S_6	5.79 214	0.013	S_9	6.22 199	0.050	P_{NO2} → π*/π → π*	5.86 212	0.420

[a] The first three excited states (S_1–S_3) are computed with the active space CAS(16,12) and states S_4–S_6 are calculated with CAS(12,11).

Table 5 MS-CASPT2/CASSCF and CC2 excitation energies ΔE (in eV and nm), oscillator strengths f, and results of the Gaussian decomposition of the experimental spectrum of p-NBA

p-NBA

MS-CASPT2/CASSCF States[a]	ΔE (eV, nm)	f	RI-CC2 States	ΔE (eV, nm)	f	Assignment	Experiment Gauss center (eV, nm)	f
S_1	3.53 352	0.000	S_1	3.83 324	0.000	n → π*	3.76 330	0.006
S_2	3.60 344	0.000	S_2	3.94 315	0.000	n → π*		
S_3	4.04 307	0.000	S_3	4.51 275	0.000	n → π*		
S_4	4.19 296	0.008	S_4	4.74 262	0.018	π → π*	4.34 286	0.028
S_5	4.85 256	0.373	S_5	5.47 227	0.454	π → π*	4.85 256	0.090
—			S_6	6.24 199	0.000	n → π*	5.06 245	0.190
							5.29 234	0.100
S_6	5.57 223	0.024	S_7	6.29 197	0.023	P_{NO2} → π*	6.08 204	0.110
			S_8	6.45 192	0.000	n → π*	6.48 191.3	—
			S_9	6.76 183	0.149	π → π*		
			S_{10}	6.89 180	0.063	π → π*		

[a] The first three excited states (S_1–S_3) are computed with the active space CAS(16,12) and states S_4–S_6 are calculated with CAS(12,11).

CC2, respectively (see Table 4). For p-NBA the experimental value is 4.34 eV_e and the calculations deliver an energy of 4.19 eV_t (MS-CASPT2) or 4.74 eV_t (CC2). This transition exhibits a (weak) vibronic progression. For all isomers the transitions involve promotions of electrons from benzene centred π orbitals to π* orbitals located at the benzene ring and the nitro group.

Going to higher energies the absorption spectra of the isomers are substantially different, requiring separated discussions of the isomers. For m-NBA, the two experimental Gaussians that decompose the band at ca. 5.3 eV_e are due to the S_5 states of both meta-conformers, at 5.02 and 5.43 eV_t (MS-CASPT2), or due to the S_6 states at 5.63 and 5.79 eV_t (CC2). Note that the CC2 method intercalates one dark nπ* state, which does

not contribute to the spectrum. The energies of the S₅ state of the two *meta*-conformers differ by about 0.4 eV (MS-CASPT2) or 0.2 eV (CC2). This energy gap is much larger than for any other transition (Table 4); this is due to the fact that the orbitals involved in these transitions are not of the same nature for both isomers. The most intense band centred at *ca.* 5.7 eV$_e$ is decomposed in terms of three Gaussians, which can be assigned with the help of CC2 to the S₇(1), S₇(2), S₉(1) and S₉(2) (S₈ is a dark nπ* state), while with MS-CASPT2 only provides one transition with the number of states calculated. These are all ππ* transitions with the participation of the nitro and carbonyl groups.

In the experimental *p*-NBA spectrum a very intense and broad absorption peaking around 4.96 eV$_e$ is recorded. The best experimental description of this band is done with three Gaussians centred at 4.85, 5.06, and 5.29 eV$_e$. However, in this spectral range the computations predict only the S₅ state at 4.85 eV$_t$ (MS-CASPT2) or the combination of the S₅ state at 5.47 eV$_t$ and a weak nπ* absorption at 6.24 eV$_t$ (CC2), see Table 5. The bright states correspond to ππ* transitions that partially involve charge transfer from the benzene ring to the nitro group. The next absorbing states contribute to the band highest in energy, which is also characterized by aromatic transitions including the P$_{NO2}$ non-bonding orbital.

In general, we observe that the excitation energies obtained with CC2 are blue-shifted with respect to MS-CASPT2 values by *ca.* 0.3 eV and 0.6 eV for the nπ* and ππ* excitations, respectively. Not surprisingly, the energy values obtained multiconfigurationally for the main peaks are in better agreement with the experiment, while the CC2 values are in many cases
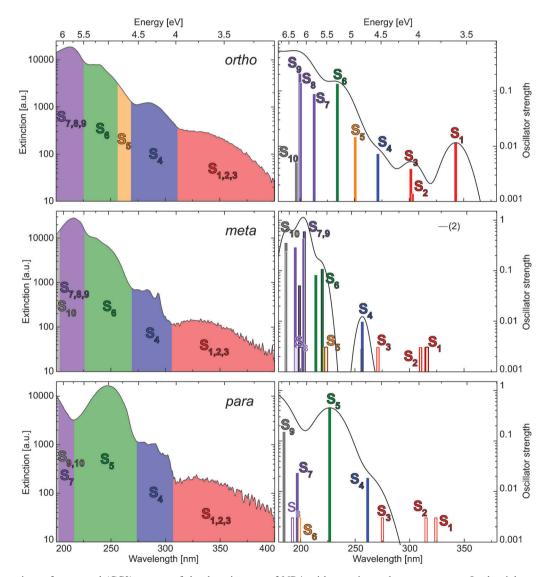

Fig. 4 Comparison of computed (CC2) spectra of the three isomers of NBA with experimental vapour spectra. In the right panels transition energies and oscillator strengths are represented by coloured bars. Since for the *m*- and *p*-NBA the calculations cannot reproduce the experimental intensity of the nπ* transitions that is due to vibronic effects, the strengths of corresponding transitions (represented by open bars) have arbitrarily been set to 0.01. The *meta*(1)-conformer of the *meta*-isomer is distinguished from the *meta*(2)-conformer by the solid black lines surrounding the bars. For the sake of comparison with the experimental data, smooth *ortho*-, *meta*- and *para*-spectra were generated by convoluting each transition with a Gaussian of 12, 5.5 and 14 nm full width at half maximum (FWHM), respectively. For the *meta*-isomer spectra of the two conformers were averaged.

overestimated. However, the single reference CC2 method, which can describe a much large number of states in a single calculation, is better suited to assign individual Gaussians, as deconvoluted from the experimental spectrum. Interestingly, the oscillator strengths predicted by CC2 are in better agreement with the intensity of the experimental bands than those calculated by MS-CASPT2. Fig. 4 (right) shows the simulated *ab initio* spectrum using CC2 excitations and oscillator strengths. Disregarding the energetic shifts, the agreement of the CC2 spectra with the experimental ones is reasonable, in particular for intense bands located at high energies. As stated above, the computations cannot reproduce the experimental intensity of the band associated with $n\pi^*$ transitions of *m*- and *p*-NBA. Therefore, only the transition energies of the lowest energy band of these two isomers can be compared with the experiments. For the non-planar *o*-NBA the computations yield (relative) transition strengths for these states in reasonable agreement with the experiment.

Finally, we discuss the solvatochromic shifts and the dipole moments of the excited states. The discussion will be restricted to the *ortho*- and *para*-isomers. The two conformers of the *meta*-isomer differ already substantially (by ~ 3 D) in their ground state dipole moments.[38] Thus, the two conformers are expected to exhibit different solvatochromic effects. In the experiment only a "superposition" of these effects is measured. The MS-CASPT2/CASSCF computation yields a dipole moment of 4.22 D for the ground state of *o*-NBA (see Table 6) close to the experimental value of 4.6 D.[39] Except for the S_4 and S_5 states the computed excited state dipole moments are slightly smaller than that of the S_0 state. The dipole moments of the excited states span angles in between $\sim 2°$ and $40°$ with the moment of the ground state. An analysis based on a Lippert–Mataga treatment[33] (data not shown) incorporating the vector character of the dipole moments shows that for all except the S_4 and S_5 states shifts to higher frequencies with increasing polarity should occur. This predication is not in line with the experiment.

Similarly, for *p*-NBA one computes a S_0 dipole moment of 2.78 D comparable to the experimental value of 2.39 D.[40] Except for the S_1 and S_5 states all moments are smaller than that of the ground state. The angles spanned by the moments cover a broader range ($2°–90°$) than the angles for *o*-NBA. A "vector" Lippert–Mataga treatment only predicts shifts to lower frequencies for the S_1 and S_5 states. In the experiment all transitions shift to lower frequencies. At present we cannot

state whether this discrepancy is due to flaws in the Lippert–Mataga treatment or to errors connected to the calculated dipole moments. In any case, one cannot rely on the solvatochromic shifts to corroborate the band assignment provided by the theoretical calculations.

6. Conclusions

The electronic absorption spectra of the three isomers *o*-, *m*-, and *p*-NBA have been analyzed, both experimentally and with the help of multiconfigurational MS-CASPT2/CASSCF and CC2 calculations. Their spectra are all characterized by weak transitions ($\varepsilon_{max} \approx 100$ M^{-1} cm^{-1}) centered around 3.5 eV. These transitions could be attributed to the promotions of electrons from n-orbitals, located at the nitro- as well as the carbonyl-function, to π^* orbitals. Stronger transitions ($\varepsilon_{max} \approx 1000$ M^{-1} cm^{-1}) at ~ 4 eV involve π- and π^*-orbitals of the benzene ring. For *m*- and *p*-NBA a faint vibronic structure is observed. At higher energies the spectra of *o*- and *m*-NBA are very similar exhibiting shoulders at ~ 5.3 eV and a peak at ~ 5.8 eV. Shoulders and peaks could be attributed to $\pi\pi^*$-transitions with a strong charge transfer (CT)-character. The *para*-isomer features a strong band at about 5 eV enclosing presumably two electronic transitions of CT-character.

The spectra of all isomers experience solvatochromic shifts of ~ -0.20 eV (gas phase $\rightarrow$ cyclohexane) and ~ -0.25 eV (gas phase $\rightarrow$ acetonitrile). The differences of the shifts induced by the various solvents are not very pronounced. Photoreactivity and stability do not show up in the UV/Vis spectra. The spectrum of the photoreactive *ortho*-isomer resembles that of the photostable *meta*-isomer. The two spectra in turn differ from the spectrum of the photostable *para*-isomer. In line with that, ultrafast fluorescence decays were recorded for all isomers.[3] In these experiments the excitation was tuned to 260 nm (4.77 eV) addressing $\pi\pi^*$ states with CT character for all isomers. These states decay within ≤ 100 fs resulting in a strong (two orders of magnitude) reduction of the fluorescence signal. This reduction is in line with the population of $n\pi^*$ states which—as this study shows—are one to two orders of magnitude weaker in oscillator strength.

Table 6 Dipole moments (in D) for *o*- and *p*-NBA of ground and excited states computed at the MS-CASPT2/CASSCF level of theory. Modulus of the moments as well as the angles (in degrees) spanned between ground and excited state moments are given

	$|\mathbf{\mu}_{ii}|/D$ *o*-NBA	Θ_{0i}/degrees	$|\mathbf{\mu}_{ii}|/D$ *p*-NBA	Θ_{0i}/degrees
S_0	4.223		2.784	
S_1	3.320	21.5	4.714	33.3
S_2	2.939	14.6	1.770	55.9
S_3	2.751	1.9	1.793	49.3
S_4	5.034	5.6	2.695	1.9
S_5	8.184	11.3	5.027	20.0
S_6	2.670	38.1	2.428	90.2

Notes and references

1 A. P. Pelliccioli and J. Wirz, *Photochem. Photobiol. Sci.*, 2002, **1**, 441.
2 S. Laimgruber, W. J. Schreier, T. Schrader, F. Koller, W. Zinth and P. Gilch, *Angew. Chem., Int. Ed.*, 2005, **44**, 7901.

3 B. Heinz, T. Schmierer, S. Laimgruber and P. Gilch, *J. Photochem. Photobiol., A*, 2008, **199**, 274.
4 S. Laimgruber, T. Schmierer, P. Gilch, K. Kiewisch and J. Neugebauer, *Phys. Chem. Chem. Phys.*, 2008, **10**, 3872.
5 T. Schmierer, W. J. Schreier, F. O. Koller, T. E. Schrader and P. Gilch, *Phys. Chem. Chem. Phys.*, 2009, **11**, 11596.
6 V. Leyva, I. Corral, T. Schmierer, B. Heinz, F. Feixas, A. Migani, L. Blancafort, P. Gilch and L. Gonzalez, *J. Phys. Chem. A*, 2008, **112**, 5046.
7 P. Coppens and G. M. J. Schmidt, *Acta Crystallogr.*, 1964, **17**, 222.
8 A. D. Becke, *J. Chem. Phys.*, 1993, **98**, 1372.
9 C. T. Lee, W. T. Yang and R. G. Parr, *Phys. Rev. B: Condens. Matter*, 1988, **37**, 785.
10 M. J. Frisch, G. W. Trucks, H. B. Schlegel, G. E. Scuseria, M. A. Robb, J. R. Cheeseman, J. A. Montgomery, T. Vreven, K. N. Kudin, J. C. Burant, J. M. Millam, S. S. Iyengar, J. Tomasi, V. Barone, B. Mennucci, M. Cossi, G. Scalmani, N. Rega, G. A. Petersson, H. Nakatsuji, M. Hada, M. Ehara, K. Toyota, R. Fukuda, J. Hasegawa, M. Ishida, T. Nakajima, Y. Honda, O. Kitao, H. Nakai, M. Klene, X. Li, J. E. Knox, H. P. Hratchian, J. B. Cross, V. Bakken, C. Adamo, J. Jaramillo, R. Gomperts, R. E. Stratmann, O. Yazyev, A. J. Austin, R. Cammi, C. Pomelli, J. W. Ochterski, P. Y. Ayala, K. Morokuma, G. A. Voth, P. Salvador, J. J. Dannenberg, V. G. Zakrzewski, S. Dapprich, A. D. Daniels, M. C. Strain, O. Farkas, D. K. Malick, A. D. Rabuck, K. Raghavachari, J. B. Foresman, J. V. Ortiz, Q. Cui, A. G. Baboul, S. Clifford, J. Cioslowski, B. B. Stefanov, G. Liu, A. Liashenko, P. Piskorz, I. Komaromi, R. L. Martin, D. J. Fox, T. Keith, A. Laham, C. Y. Peng, A. Nanayakkara, M. Challacombe, P. M. W. Gill, B. Johnson, W. Chen, M. W. Wong, C. Gonzalez and J. A. Pople, *Gaussian 03, Revision C.02*, Gaussian, Inc., Wallingford CT, 2004.
11 F. M. Bickelhaupt and E. J. Baerends, *Rev. Comput. Chem.*, 2000, **15**, 1.
12 G. te Velde, F. M. Bickelhaupt, E. J. Baerends, S. J. A. van Gisbergen, C. Fonseca Guerra, J. G. Snijders and T. Ziegler, *J. Comput. Chem.*, 2001, **22**, 931.
13 T. Ziegler and A. Rauk, *Theor. Chim. Acta*, 1977, **46**, 1.
14 K. Morokuma, *J. Chem. Phys.*, 1971, **55**, 1236.
15 A. Kovács, C. Esterhuysen and G. Frenking, *Chem.–Eur. J.*, 2005, **11**, 1813.
16 I. Fernández and G. Frenking, *J. Org. Chem.*, 2006, **71**, 2251.
17 A. D. Becke, *J. Phys. Chem. A*, 1988, **38**, 3098.
18 J. P. Perdew, *J. Phys. Chem. B*, 1986, **33**, 8822.
19 J. G. Snijders, E. J. Baerends and P. Vernooijs, *At. Data Nucl. Data Tables*, 1982, **26**, 483.
20 C. Fonseca Guerra, J. G. Snijders, G. te Velde and E. J. Baerends, *Theor. Chem. Acc.*, 1998, **99**, 391.
21 E. J. Baerends, J. Autschbach, D. Bashford, A. Bérces, F. M. Bickelhaupt, C. Bo, P. M. Boerrigter, L. Cavallo, D. P. Chong, L. Deng, R. M. Dickson, D. E. Ellis, M. van Faassen, L. Fan, T. H. Fischer, C. Fonseca Guerra, A. Ghysels, A. Giammona, S. J. A. van Gisbergen, A. W. Götz, J. A. Groeneveld, O. V. Gritsenko, M. Grüning, F. E. Harris, P. van den Hoek, C. R. Jacob, H. Jacobsen, L. Jensen, G. van Kessel, F. Kootstra, M. V. Krykunov, E. van Lenthe, D. A. McCormack, A. Michalak, M. Mitoraj, J. Neugebauer, V. P. Nicu, L. Noodleman, V. P. Osinga, S. Patchkovskii, P. H. T. Philipsen, D. Post, C. C. Pye, W. Ravenek, J. I. Rodríguez, P. Ros, P. R. T. Schipper, G. Schreckenbach, M. Seth, J. G. Snijders, M. Solà, M. Swart, D. Swerhone, G. te Velde, P. Vernooijs, L. Versluis, L. Visscher, O. Visser, F. Wang, T. A. Wesolowski, E. M. van Wezenbeek, G. Wiesenekker, S. K. Wolff, T. K. Woo, A. L. Yakovlev and T. Ziegler, ADF2009.01, SCM, Theoretical Chemistry, Vrije Universiteit, Amsterdam, The Netherlands, 2009, http://www.scm.com.
22 O. Christiansen, H. Koch and P. Jorgensen, *Chem. Phys. Lett.*, 1995, **243**, 409.
23 J. Finley, P. A. Malmqvist, B. O. Roos and L. Serrano-Andres, *Chem. Phys. Lett.*, 1998, **288**, 299.
24 B. O. Roos, *Ab initio Methods in Quantum Chemistry II*, ed. K. P. Lawley, Wiley, Chichester, 1987.
25 I. Corral and L. González, *J. Comput. Chem.*, 2008, **29**, 1982.
26 B. O. Roos and K. Andersson, *Chem. Phys. Lett.*, 1995, **245**, 215.
27 P. A. Malmqvist and B. O. Roos, *Chem. Phys. Lett.*, 1989, **155**, 189.
28 P. O. Widmark, P. A. Malmqvist and B. O. Roos, *Theoret. Chim. Acta*, 1990, **77**, 291.
29 G. Karlström, R. Lindh, P. Å. Malmqvist, B. O. Roos, U. Ryde, V. Veryazov, P. O. Widmark, M. Cossi, B. Schimmelpfennig and P. N. a. L. Seijo, *Comput. Mater. Sci.*, 2003, **28**, 222.
30 R. Ahlrichs, M. Bär, M. Häser, H. Horn and C. Kölmel, *Chem. Phys. Lett.*, 1989, **162**, 165.
31 D. B. Galloway, J. A. Bartz, L. G. Huey and F. F. Crim, *J. Chem. Phys.*, 1993, **98**, 2107.
32 N. J. Turro, V. Ramamurthy and J. C. Scaiano, *Principles of Molecular Photochemistry: An Introduction*, University Science Books, Sausalito, 2009.
33 J. R. Lakowicz, *Principles of Fluorescence Spectroscopy*, Springer, New York, 3rd edn, 2006.
34 J. A. King and G. L. Bryant, *Acta Crystallogr., Sect, C: Cryst. Struct. Commun.*, 1996, **52**, 1691.
35 P. Coppens, *Acta Crystallogr.*, 1964, **17**, 573.
36 S. Pinchas, *Anal. Chem.*, 1957, **29**, 334.
37 V. Leyva, I. Corral and L. Gonzalez, *Z. Phys. Chem.*, 2008, **222**, 1263.
38 A. Konopacka, J. Kalenik and Z. Pawelka, *J. Molec. Struct.*, 2004, **705**, 75.
39 R. J. Sengwa and K. Kaur, *Indian J. Phys., B*, 1999, **73**, 493.
40 C. T. Aw, E. L. K. Tan and H. H. Huang, *J. Chem. Soc., Perkin Trans. 2*, 1972, 1638.